doi:10.1093/brain/awl125 *Brain* (2006), **129**, 1892–1906

Periventricular heterotopia: phenotypic heterogeneity and correlation with *Filamin A* mutations

E. Parrini,[1]* A. Ramazzotti,[1]* W. B. Dobyns,[12] D. Mei,[1] F. Moro,[1] P. Veggiotti,[3] C. Marini,[1] E. H. Brilstra,[16] B. Dalla Bernardina,[4] L. Goodwin,[17] A. Bodell,[9] M. C. Jones,[13] M. Nangeroni,[5] S. Palmeri,[6] E. Said,[18] J. W. Sander,[14] P. Striano,[7] Y. Takahashi,[19] L. Van Maldergem,[20] G. Leonardi,[8] M. Wright,[15] C. A. Walsh[10,11] and R. Guerrini[1,2]

[1]Research Institute I.R.C.C.S. Stella Maris Foundation and [2]Department of Child Neurology and Psychiatry, University of Pisa, [3]Child Neuropsychiatry Department, Neurological Institute Casimiro Mondino Foundation I.R.C.C.S., University of Pavia, [4]Department of Pediatrics and Child Neuropsychiatry, Verona University Medical School, [5]E. Agnelli Hospital, Pinerolo, Torino, [6]Department of Neurological and Behavioural Sciences, University of Siena, [7]Department of Neurological Sciences, University of Napoli Federico II, [8]Unit of Child Neurology and Psychiatry Fatebenefratelli Hospital, Milano, Italy, [9]Walsh Laboratory, Harvard Medical School, [10]Division of Neurogenetics and Howard Hughes Medical Institute, Department of Neurology, Beth Israel Deaconess Medical Center, Harvard Medical School, [11]Program in Biological and Biomedical Sciences, Harvard Medical School, Boston, MD, [12]Department of Human Genetics, Neurology and Pediatrics, University of Chicago, IL, [13]Children Hospital and Health Centre, San Diego, CA, USA, [14]Department of Clinical and Experimental Epilepsy, Institute of Neurology, London, [15]Institute of Human Genetics International Centre for Life, Newcastle-upon-Tyne, UK, [16]Department of Medical Genetics, University Medical Center, Utrecht, The Netherlands, [17]Department of Genetics, Nepean Hospital, Penrith, Australia, [18]St Luke's Hospital, Gwardamangia, Malta, [19]National Epilepsy Centre, Shizuoka Medical Institute of Neurological Disorders, Shizuoka, Japan and [20]Human Genetics Centre, Institute of Pathology and Genetics-Loverval, Belgium

*These authors contributed equally to this work.

Correspondence to: Prof. Renzo Guerrini, Division of Child Neurology and Psychiatry I.R.C.C.S. Stella Maris Foundation, University of Pisa-via dei Giacinti, 2-56018 Calambrone, Pisa, Italy E-mail: renzo.guerrini@inpe.unipi.it

Periventricular heterotopia (PH) occurs when collections of neurons lay along the lateral ventricles or just beneath. Human *Filamin A* gene (*FLNA*) mutations are associated with classical X-linked bilateral periventricular nodular heterotopia (PNH), featuring contiguous heterotopic nodules, mega cisterna magna, cardiovascular malformations and epilepsy. *FLNA* encodes an F-actin-binding cytoplasmic phosphoprotein and is involved in early brain neurogenesis and neuronal migration. A rare, recessive form of bilateral PNH with microcephaly and severe delay is associated with mutations of the *ADP-ribosylation factor guanine nucleotide-exchange factor-2* (*ARFGEF2*) gene, required for vesicle and membrane trafficking from the trans-Golgi. However, PH is a heterogeneous disorder.We studied clinical and brain MRI of 182 patients with PH and, based on its anatomic distribution and associated birth defects, identified 15 subtypes. Classical bilateral PNH represented the largest group (98 patients: 54%). The 14 additional phenotypes (84 patients: 46%) included PNH with Ehlers–Danlos syndrome (EDS), temporo-occipital PNH with hippocampal malformation and cerebellar hypoplasia, PNH with fronto-perisylvian or temporo-occipital polymicrogyria, posterior PNH with hydrocephalus, PNH with microcephaly, PNH with frontonasal dysplasia, PNH with limb abnormalities, PNH with fragile-X syndrome, PNH with ambiguous genitalia, micronodular PH, unilateral PNH, laminar ribbon-like and linear PH. We performed mutation analysis of *FLNA* in 120 patients, of whom 72 (60%) had classical bilateral PNH and 48 (40%) other PH phenotypes, and identified 25 mutations in 40 individuals. Sixteen mutations had not been reported previously. Mutations were found in 35 patients with classical bilateral PNH, in three with PNH with EDS and in two with unilateral PNH. Twenty one mutations were nonsense and frame-shift and four missense. The high prevalence of mutations causing protein truncations confirms that loss of function is the major cause of the disorder. *FLNA* mutations were found in 100% of familial cases with X-linked PNH (10 families: 8 with classical bilateral PNH,

1 with EDS and 1 with unilateral PH) and in 26% of sporadic patients with classical bilateral PNH. Overall, mutations occurred in 49% of individuals with classical bilateral PNH irrespective of their being familial or sporadic. However, the chances of finding a mutation were exceedingly gender biased with 93% of mutations occurring in females and 7% in males. The probability of finding *FLNA* mutations in other phenotypes was 4% but was limited to the minor variants of PNH with EDS and unilateral PNH. Statistical analysis considering all 42 mutations described so far identifies a hotspot region for PNH in the actin-binding domain ($P < 0.05$).

Keywords: periventricular heterotopia; filamin A; *FLNA*; mutation; genetic counselling

Abbreviations: CH = calponin homology; DHPLC = denaturing high performance liquid chromatography; EDS = Ehlers–Danlos syndrome; NMD = nonsense-mediated mRNA decay; OPD = otopalatodigital; PH = periventricular heterotopia; PMG = polymicrogyria; PNH = periventricular nodular heterotopia; RT–PCR = reverse transcription–polymerase chain reaction

Received January 18, 2006. Revised April 1, 2006. Accepted April 10, 2006. Advance Access publication May 9, 2006

Introduction

Defects of the human *Filamin A* gene (*FLNA*; chromosomal locus Xq28) cause X-linked periventricular nodular heterotopia (PNH; OMIM 300049) (Eksioglu *et al.*, 1996; Fox *et al.*, 1998), a malformation of neuronal migration (Barkovich *et al.*, 1992) characterized by nodules of neurons in an inappropriate location adjacent to the walls of the lateral ventricles, the location of the embryonic ventricular zone (Dobyns *et al.*, 1996). PNH can be bilateral or unilateral. Periventricular heterotopia (PH) may also be laminar, rather than nodular. Most patients with PH have seizures whose severity and age at onset are variable (Huttenlocher *et al.*, 1994; Guerrini and Carrozzo, 2001).

PNH may also be observed in patients with chromosomal rearrangements, such as duplication of 5p15.1 or 5p15.33 (Sheen *et al.*, 2003*b*), or with mutations of *ARFGEF2*, which cause a rare autosomal recessive syndrome of PNH and microcephaly (Sheen *et al.*, 2004*a*). PNH has also been associated with hydrocephalus (Sheen *et al.*, 2004*b*), frontonasal malformation (Guerrini and Dobyns, 1998), severe mental retardation and syndactyly (Dobyns *et al.*, 1997; Fink *et al.*, 1997), Ehlers–Danlos syndrome (EDS) (Thomas *et al.*, 1996; Sheen *et al.*, 2005) or nephrosis (Palm *et al.*, 1986). Whether each of these variants represents a truly distinct compound disorder with a specific genetic mechanism remains to be determined.

FLNA codes for the F-actin-binding cytoplasmic cross-linking phosphoprotein filamin A (FLNA) (Carroll *et al.*, 1982; Chen *et al.*, 1989), composed of three major functional domains: an actin binding domain (ABD), at the N-terminus, consisting of tandem pairs of calponin homology domains (CH1 and CH2), a rod domain consisting of 23 immunoglobulin-like repeats interrupted by two hinge regions ('hinge 1' and 'hinge 2') and a C-terminal domain, which is important for dimerization and binding to several membrane receptors (Noegel *et al.*, 1989; Gorlin *et al.*, 1990; Hock *et al.*, 1990).

The specific roles of filamin A and its association with pathological conditions are still to be fully understood. Additional functional complexity is conferred by the existence and by the time/tissue-specific expression of the two human paralogous genes *Filamin B* and *Filamin C* (Stossel *et al.*, 2001; van der Flier and Sonnenberg, 2001). The Y-shaped homodimerized *FLNA* promotes the organization of actin filaments in orthogonal networks of the cytoskeleton. A similar mechanism might also be hypothesized for filamin B and C, even if their heterodimerization has been demonstrated only *in vitro* (Himmel *et al.*, 2003). In addition, filamin A and filamin B co-localize within neuronal precursors and heterodimerization of these two isoforms has been hypothesized (Sheen *et al.*, 2002). Interactions of the dimer with integrin receptors, transmembrane proteins and several signalling proteins are believed to integrate extracellular and cytoplasmic signals with cellular cytoskeleton rearrangements and membrane reshaping (Meyer *et al.*, 1997; Loo *et al.*, 1998; Ott *et al.*, 1998; Dulabon *et al.*, 2000; Tu *et al.*, 2003). Filamin homologues have been shown to be implicated in regulation of cell stability, protrusion and motility across various biological systems (Stendahl *et al.*, 1980; Cunningham, 1995; Ott *et al.*, 1998). The mouse *Filamin A* orthologue was abundantly expressed in the cell soma and leading processes of migratory neurons and is widely distributed across the cortical mantle, reaching the highest levels in the ventricular zone within the cortex during neurogenesis (Sheen *et al.*, 2002). FLNA likely influences neuroblast migration during cortical development in vertebrates, and PH in humans likely results from disruption of this process (Sheen *et al.*, 2001).

Mutations of the *FLNA* gene have also been associated with the otopalatodigital (OPD) syndrome spectrum, which includes OPD I (OPD1; OMIM 311300) and OPD II (OPD2; OMIM 304120), frontometaphyseal dysplasia (FMD; OMIM 305620) and Melnick-Needles syndrome (MNS; OMIM 309350) (Robertson *et al.*, 2003).

Since 1998, 45 mutations of *FLNA* have been reported in patients with PNH or the OPD syndrome spectrum (Robertson *et al.*, 2003; Hidalgo-Bravo *et al.*, 2005;

Stefanova *et al.*, 2005), including 25 missense, 3 nonsense and 8 splice site mutations, plus 7 deletions and 2 insertions (mutations related to PNH are summarized in Table A as Supplementary online material). To extend these observations, we have reviewed clinical and brain imaging data in 182 individuals with PH, and identified 25 *FLNA* mutations including 16 novel mutations in 40 of the 120 patients tested. We report genotype–phenotype analysis in these 40 patients, and describe 15 clinically distinct subgroups including 3 associated with *FLNA* mutations in many but not all patients, 4 previously reported syndromes (Guerrini and Dobyns, 1998; Sheen *et al.*, 2004*a*; Wieck *et al.*, 2005), and 8 novel phenotypes.

Patients and methods

Clinical information, brain MRI and PH subclasses

Clinical information and brain MRI of 182 patients with PH were either collected at the Division of Child Neurology and Psychiatry, University of Pisa, or obtained from the patients' referring hospitals. Informed consents were obtained from the respective human subject institutional review boards. We collected clinical information and assessed brain MRI for the purpose of classifying patients. We analysed the shape, location and symmetry of PH; the presence of any associated brain malformations or other congenital anomalies; and specific syndrome diagnosis (Table 1).

Seventeen patients were included in the 'unclassified' group because either neuroimaging was just sufficient to detect PH, but not clear enough to fully characterized its extent and morphology, or clinical information was insufficient for delineating a syndrome category.

Once the phenotype characterization was obtained using the criteria described above, we performed mutation analysis of the *FLNA* gene in subsets of patients belonging to most of the phenotypic subclasses and analysed the rate of mutations according to specific phenotype, familial or sporadic occurrence and gender.

Genomic DNA samples

Genomic DNA of 120 individuals with PH (64 women and 56 men) was extracted from peripheral blood leucocytes using a DNA isolation kit (DNAzol, MRC, Cincinnati, OH, USA).

Molecular analysis of *FLNA*

We carried out mutation screening of the coding regions of *FLNA* (Gen Bank accession number NM_ 002834) by denaturing high performance liquid chromatography (DHPLC), according to the manufacturer's specifications (Transgenomics, La Jolla, CA, USA). The 47 exons covering coding regions and their respective upstream and downstream intron–exon boundaries were amplified by PCR. Primer sequences, PCR conditions and DHPLC analysis temperatures are available on request. Amplicons from male subjects were mixed with half volume of PCR product of the same *FLNA* region amplified by the same conditions from an unaffected female DNA. PCR products that showed an alteration in the DHPLC elution profile were purified using the GenElute PCR clean-up kit (Sigma Aldrich, Italy) and cycle sequenced on both strands using the BigDye Terminator v1.1 chemistry (Applied Biosystems, Foster City, CA, USA) and an ABI3100-Avant automated sequencer (Applied Biosystems). The nucleotide changes observed (*see* Results) were not found in 125 DNA samples of mixed ethnic origin.

For Patient 2a, who carries a silent mutation in exon 31 (Table 2), we used the Berkeley Drosophila Genome Project (BDGP) splice database (http://www.fruitfly.org/seq_tools/splice.html) to predict *in silico* whether the nucleotide change would alter the mRNA splicing of exon 31, its neighbouring exons, or both. Total RNA was isolated from a lymphoblastoid cell line using the GenElute mammalian total RNA kit (Sigma Aldrich, Italy). Reverse transcription (RT) was performed using 1 μg total RNA with random hexanucleotide primers and Im ProM-II Reverse Transcriptase (Promega, Italy). The cDNA was amplified by the following primer pair: F31-RT-F (5′-ctgtggacactaaggcggc-3′)–F32-RT-R (5′-gctgctgagaccgtagagg-3′); the RT product was then sequenced as described above. In order to assess nonsense-mediated mRNA decay (NMD), RT–PCR was performed on the patient's lymphoblastoid cell line treated for 24 h with 100 μg/ml cycloheximide, an NMD inhibitor, as previously described (Usuki *et al.*, 2004). RT–PCR products were cloned into the pGEM-T-easy vector (Promega, Italy) according to the manufacturer's protocol. The resulting colonies were amplified with primers (T7 and SP6) flanking the vector's poly-cloning site and verified for the presence of inserted fragments by gel electrophoresis.

In the same patient we also tested the pattern of X-chromosome inactivation with the androgen receptor (AR) assay, using a fluorescence-labelled primer on leucocyte-derived DNA (Allen *et al.*, 1992). The PCR products were analysed on an ABI PRISM 3100 Avant genetic sequencer, and the allele sizes were determined by GENEMAPPER software (Applied Biosystems).

Patient 6a carried a substitution of 2 nt in exon 25 (Table 2). To verify whether such changes were in *cis* or in a *trans* configuration, we subcloned the PCR product of exon 25 obtained from genomic DNA into the pGEM-T-easy vector (Promega, Italy) and subsequently sequenced the resulting insert using T7 and SP6 primers.

Statistical analysis

To establish whether *FLNA* contains mutational hotspots, we performed statistical analysis considering all 42 mutations described so far, including the 16 new mutations reported herein. Mutations were tabulated according to their location in the gene, considering the coding exons plus the 10 nt upstream and downstream from each exon: ABD (904 nt), Rod domain 1 + Hinge 1 region (5029 nt), Rod domain 2 + Hinge 2 (2629 nt) and C-terminal domain (299 nt). For comparison, Fisher's exact test was applied to verify the hypothesis of absence of hotspot regions for *FLNA* mutations, taking into account the relative sizes of the four domains. Fisher's exact test is a method of performing inference in two-way contingency tables using exact distributions.

We applied the χ^2 test with one degree of freedom to establish if significant skewing of the sex ratio occurred in patients with classical bilateral PNH but no mutations of the *FLNA* gene.

Results

PH subclasses

Based on the comparison of clinical and brain MRI findings of the 182 patients, we defined 15 phenotypic subclasses

Table 1 PH classes, patients and *FLNA* analysis

Shape	Location	Associated malformations/syndromes	Figure no.	Patients (no.)	♂	♀	*FLNA* analysis	Mutations (no.)	Sporadic (no.)	Familial (no.)	Relatives with mutations (no.)
1. Nodular	1.1. Bilateral diffuse	1.1.1 With frontonasal dysplasia	(3C–D)	7	6	1	6				
	1.2. Bilateral diffuse sparing	1.2.1. 'Classical' bilateral PNH	(1)	98	44	54	72	21+1*	13	8	13+1*
		1.2.2. With Ehlers–Danlos syndrome	(1)	3	0	3	3	3*	2	1	0*
		1.2.3. With micronodules		2	2	0	2				
		1.2.4. With ambiguous genitalia		1	0	1	1				
		1.2.5. With limb abnormalities	(4A–B)	6	3	3	3				
		1.2.6. With microcephaly		2	1	1	2				
	1.3. Bilateral temporo-occipital and trigones	1.3.1. With polymicrogyria		2	2	0	2				
		1.3.2. With cerebellar hypoplasia	(2)	10	3	7	7				
		1.3.3. With hydrocephalus	(3B)	5	3	2	3				
	1.4. Bilateral anterior, frontal → to trigones	1.4.1. Fronto-perisylvian	(3A)	7	6	1	3				
	1.5. Unilateral diffuse sparing temporal horns		(1)	15	7	8	10	1	0	1	1
	1.6. Unilateral/bilateral isolated nodules	1.6.1. Fragile-X		2	2	0	0				
2. Laminar	2.1. Diffuse linear		(4C)	3	2	1	3				
	2.2. Posterior ribbon-like		(4D–E)	2	1	1	0				
3. Unclassified				17	10	7	3				
TOTAL				182			120	25	15	10	15

*A proband had *BPNH associated with EDS*, however, her mother had *'classical' BPNH*.

Table 2 Clinical features of patients with PH and new *FLNA* mutations

Mutation	Patient	Gender	Age (Years)	Sequence variation	Exon	Protein	Location in protein	Seizures; age at onset	Cognitive level
Splice site	1	F	8	IVS5 +2 T→A	4		repeat 1—rod 1	Yes; 6	Normal
	2a	F	20	c.5327 C→T	31		repeat 15—rod 1	No	Normal
	2b	F	24	c.5327 C→T	31		repeat 15—rod 1	No	Normal
	3	F	16	IVS44 –2 A→G	45		repeat 22—rod 2	Yes; 14,5	Normal
	4	F	48	IVS47 +8 A→G	47		repeat 24	Yes; 19	Normal
Truncating	5	F	4	c.676 C→T	4	R226X	CHD2	Yes; 2	u
	6a	F	15	c.2002 C→T	13	Q668X	repeat 4—rod 1	u	u
	6b	F	u	c.2002 C→T	13	Q668X	repeat 4—rod 1	u	u
	7a	F	32	c.[4437 A→G;4438 C→A]	25	Y1479X	repeat 12—rod 1	No	Normal
	7b	F	33	c.[4437 A→G;4438 C→A]	25	Y1479X	repeat 12—rod 1	Yes; 28	Normal
	7c	F	25	c.[4437 A→G;4438 C→A]	25	Y1479X	repeat 12—rod 1	Yes; 21	Normal
	7d	F	u	c.[4437 A→G;4438 C→A]	25	Y1479X	repeat 12—rod 1	No	Normal
	8	F	u	c.4543 C→T	27	R1515X	repeat 13—rod 1	Yes; 25	u
	9a	F	49	c.6724 C→T	41	R2242X	repeat 21—rod 2	Yes; 21	Normal
	10	F	6	c.698delA	4	fsX258	CHD2	u	u
	11a	F	25	c.4038delG	24	fsX1349	repeat 11—rod 1	Yes; 17	Normal
Deletion	11b	F	55	c.4038delG	24	fsX1349	repeat 11—rod 1	Yes; 17	Normal
	12	F	u	c.4970delG	31	fsX1671	repeat 15—rod 1	Yes; 23	Normal
	13	F	28	c.7333delG	45	fsX2452	repeat 23	Yes; 9	Normal
	14	F	u	c.7790_7803del	48	fsX2617	repeat 24	u	u
Insertion	15	F	23	c.6287_6288insAA	39	fsX2133	repeat 22—rod2	Yes; 15	Mild deficit
	16	F	8	c.7800_7801insC	48	fsX2600	repeat 24	Yes; 3	Normal

u = unknown.

of PH whose anatomical characteristics are summarized in Table 1 and Figs 1–4. Ninety-eight patients (54%) had classical bilateral PNH. Of the remaining 84 (46%) patients, 26 (31%) had bilateral PNH associated with other brain malformations, 19 (23%) had bilateral PNH associated with non-neurological abnormalities and 22 (26%) had either unilateral PNH, micronodules or laminar heterotopia. In most phenotypic subclasses the morphological characteristics of PH appeared to be sufficiently specific. The remaining 17 (20%) had different forms of PNH that did not fit features of any specific subclass.

Classical bilateral PNH

Ninety-eight patients (54 females, 44 males; age range: 2–64 years; mean age: 20 years) had bilateral symmetric nodules of grey matter lining the lateral ventricles, especially the frontal horns and ventricular bodies, with limited extension in the occipital horns, almost always sparing the temporal horns (Fig. 1A–E), or with minor temporal involvement, which, however, was never accompanied by abnormal hippocampal morphology. In 22 patients (8 probands) (22.4%) the disorder was familial, always with a pattern suggesting X-linked inheritance.

Most patients in this group had normal intelligence or mild mental retardation. Three patients, none having *FLNA* mutations, had moderate to severe mental retardation.

Epilepsy was observed in 73 patients (72%). Age at seizure onset varied from the neonatal period to 43 years (mean 12 years). Several different seizure types were observed, with most patients having focal epilepsy. Seven patients had early epileptic encephalopathies with infantile spasms and tonic seizures. Seizures were well controlled or rare in 82% of those with epilepsy.

Mutations of the *FLNA* gene were observed in 35 (49%) of the 72 patients who were tested, including 33 (77%) of 43 females and 2 (7%) of 29 males. Almost all patients with *FLNA* mutations had mild to moderate cerebellar vermis hypoplasia, and many also had cardiovascular abnormalities. In particular, twenty patients had either insufficiency of the aortic valve, patent ductus arteriosus (PDA) or idiopathic thrombocytopenia, or an association of them. Beside these abnormalities, no remarkable clinical or anatomical differences were detected between patients with or without *FLNA* mutations.

Bilateral posterior PNH (temporal horns, trigones and occipital horns) with hippocampal malformation and cerebellar hypoplasia

Ten patients (7 females, 3 males; age range: 5–50 years; mean age: 25 years) had bilateral PNH with nodules restricted to the trigones and temporal and occipital horns. Heterotopia surrounded the hippocampi that were under-rotated and rounded (Fig. 2A and B). The number of patients is too small to estimate gender ratio. All patients were sporadic with no reported consanguinity. All 10 had severe cerebellar vermis hypoplasia, and 8 had moderate to severe hypoplasia of the cerebellar hemispheres as well (Fig. 2C–E). Two

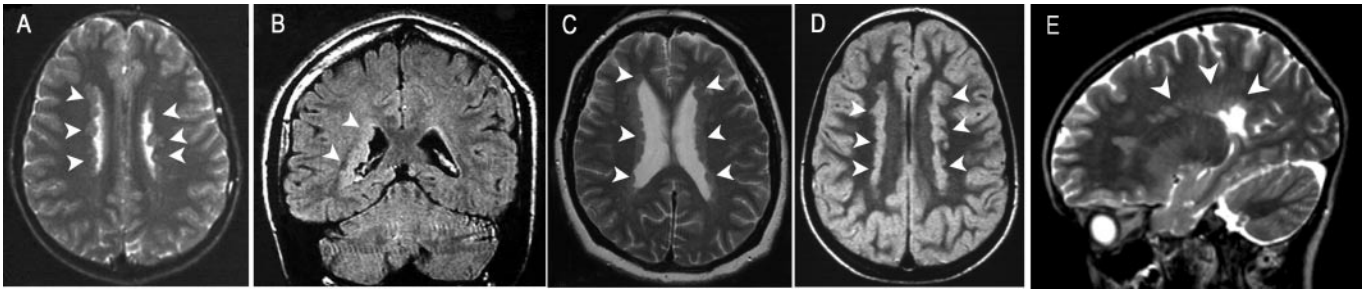

Fig. 1 Brain imaging in five females with *FLNA* mutations demonstrates extensive contiguous (**B, C, D**) or non-contiguous (**A**) PNH involving the body and trigones of the lateral ventricles with overlying normal cortex, except that heterotopia are seen only on the right in one patient (**B**). The sagittal section (**E**) shows extensive heterotopia beneath the walls of the body and trigones of the lateral ventricle, with sparing of the temporal horn and hippocampal formation. The associated *FLNA* mutations in these patients are: Q668X in patient 2-II.2 (**A**), S149P in patient 2-III.1 (as reported in Guerrini *et al*., 2004) (**B**), c.4038 delG in patient 5-I.2 (**C**) who is the mother of 5-II.2, A39G in patient F8 who has EDS (**D**), and IVS5+2T→A in Patient 1 (**E**).

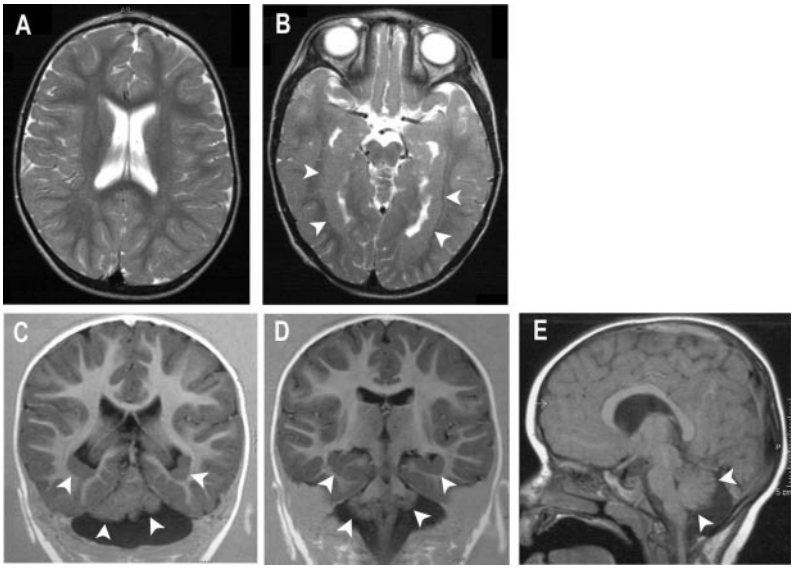

Fig. 2 Brain imaging in two patients with bilateral PNH involving the temporo-occipital horns and trigones with hippocampal malformation and cerebellar hypoplasia. **A**–**D** are from the same patient, a 6-year-old, girl. A sagittal section through the bodies of the lateral ventricles (**A**), shows that there is no subependymal heterotopia at this level; a lower sagittal section, through the temporal horns (**B**) shows contiguous bilateral subependymal heterotopia (arrowheads) which reaches the tip of the temporal horns where it merges with the hippocampal formations. Coronal sections show heterotopia surrounding the trigones (**C**) and merging with the hippocampal formation (**D**) as well as severe cerebellar hypoplasia. A sagittal section in a 15-year-old, girl (**E**), shows severe cerebellar hypoplasia involving both cerebellar hemispheres and the vermis (**C** and **D**).

patients had agenesis of the corpus callosum and four had thinning of the corpus callosum. Cerebellar signs were present in all, though their severity varied from a severe cerebellar syndrome that initially prompted brain imaging in most patients to mild dysmetria, nystagmus and dysarthria. Seven patients had epilepsy, which was always focal. Age at seizure onset ranged from 1 to 33 years (mean age: 13 years). Five patients were seizure free or had occasional seizures and the remaining 2 had uncontrolled seizures. Cognitive level varied from normal to mildly impaired. No mutations of the *FLNA* gene were observed in the 7 patients analysed.

Bilateral posterior PNH and polymicrogyria

In two boys, mostly non-contiguous PNH lining the posterior bodies, trigones and temporal and occipital horns were associated with overlying polymicrogyria (PMG) involving the temporal, parietal and occipital lobes. A series of 20 such patients (15 males and 5 females) was reported in a companion paper (Wieck *et al*., 2005). All had developmental delay and mental retardation, and most had epilepsy but the severity was variable. Both patients in this paper (and all in the companion paper) were sporadic with no reported consanguinity.

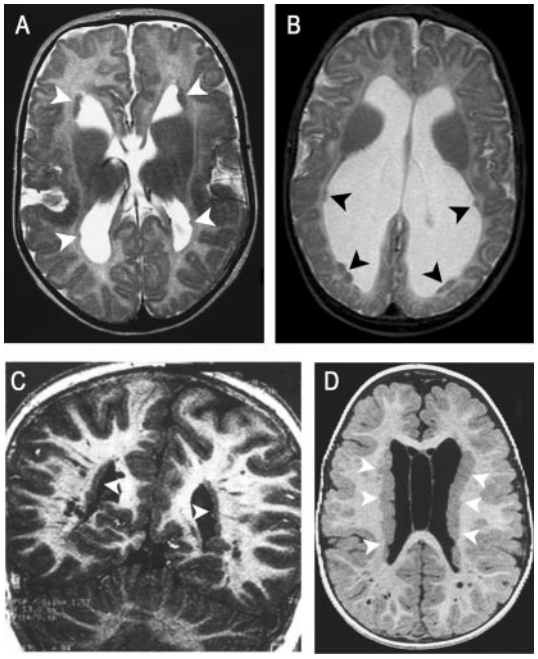

Fig. 3 Brain imaging in four children with different forms of PNH. In **A**, axial section showing bilateral PNH with fronto-perisylvian polymicrogyria in a 4-year-old boy. Small subependymal nodules are visible in both frontal and occipital horns (arrows). There is polymicrogyria in the perisylvian and fronto-opercular cortex bilaterally. In **B**, axial section in a 6-year-old boy with PNH and hydrocephalus. There is severe enlargement of both lateral ventricles, especially involving the occipital horns where small clusters of subependymal nodules are present (arrowheads). **C** and **D** are coronal and axial sections in two 7-years-old boys with bilateral PNH with frontonasal dysplasia. Both children present bilateral contiguous subependymal nodules (arrowheads) and structural abnormality in the white matter where scattered cystic formations are present, possibly representing dilated Virchow-Robin spaces.

Bilateral frontal-perisylvian PNH and polymicrogyria

In seven patients (6 males, 1 female), small and mostly non-contiguous nodules lining the frontal horns, bodies of the lateral ventricles and the trigones were associated with overlying frontal and perisylvian PMG, occasionally extending to the parietal cortex (Fig. 3A). All patients were sporadic and no consanguinity was reported in their families. Severe developmental delay, present in all, was accompanied in most by early onset seizures. No *FLNA* mutations were found in the four patients tested. Four of the patients in this group were also included in the companion paper by Wieck *et al.* (2005); three additional patients had not been reported before. The clinical characteristics of our seven patients are similar to those described in detail in Wieck's series. Combining the new patients included here and those previously reported, the male to female rate is 9 to 2, which confirms a significant skewing of the sex ratio (χ^2 test: $P = 0.034$).

Bilateral posterior PNH with hydrocephalus

Five patients (3 males, 2 females; age range: 3–35 years; mean age: 11 years) had small non-contiguous nodules or small clusters of nodules in the occipital and posterior temporal horns and trigones in association with hydrocephalus (Fig. 3B). In two unrelated patients, PNH but not hydrocephalus was present in other family members (Sheen *et al.*, 2004*b*; Family 2-III.1 and Family 3-II.3) who were not included in this study. Another patient had Chiari malformation type 1 with caudally-displaced cerebellar tonsils, syringomyelia and tethered cord. Four patients had severe developmental delay, three had epilepsy, two had spastic quadriparesis and one had PDA. Mutation analysis of *FLNA* was negative in the three patients studied.

Bilateral PNH with microcephaly

Two siblings, a boy and a girl from a Turkish, consanguineous family, had bilateral diffuse PNH, sparing the temporal horns, associated with microcephaly with head circumference – 2 SD. These two patients were included in the paper describing mutations of the *ARFGEF2* gene in recessive PNH with microcephaly (Family 2 in Sheen *et al.*, 2004*a*). Both children had severe developmental delay, spastic quadriparesis and early-onset refractory infantile spasms with hypsarrhythmia. The boy died of pneumonia at the age of 13 years.

Bilateral PNH with frontonasal dysplasia

Seven patients (6 boys, 1 girl; age range: 5–22 years; mean age: 11 years) had bilateral heterotopic nodules that were diffuse, lining the lateral ventricles. Brain MRI showed multiple cystic areas in the hemispheric white matter (Fig. 3C and D). Partial agenesis of the corpus callosum was observed in three. All seven patients had severe hypertelorism with inner and outer canthal distances above the 97th percentile, broad nasal root, poorly formed nasal tip, widow's peak and mild mental retardation; three had focal epilepsy. Two boys in this group were reported in the original description of the PNH frontonasal malformation syndrome (Guerrini and Dobyns, 1998). The five additional patients had overlapping characteristics, confirming the specificity of this syndrome. All patients were sporadic. Mutation analysis of *FLNA*, performed in six patients, gave negative results.

Bilateral PNH with limb abnormalities

Six patients (3 males, 3 females) had diffuse bilateral PNH sparing the temporal horns, similar to classical bilateral PNH (Fig. 4A), associated with limb abnormalities. However, abnormalities of limbs had different characteristics, possibly corresponding to two phenotypic subgroups. Four patients (1 male, 3 female) had limb reduction abnormalities, with missing or hypoplastic phalanges of toes

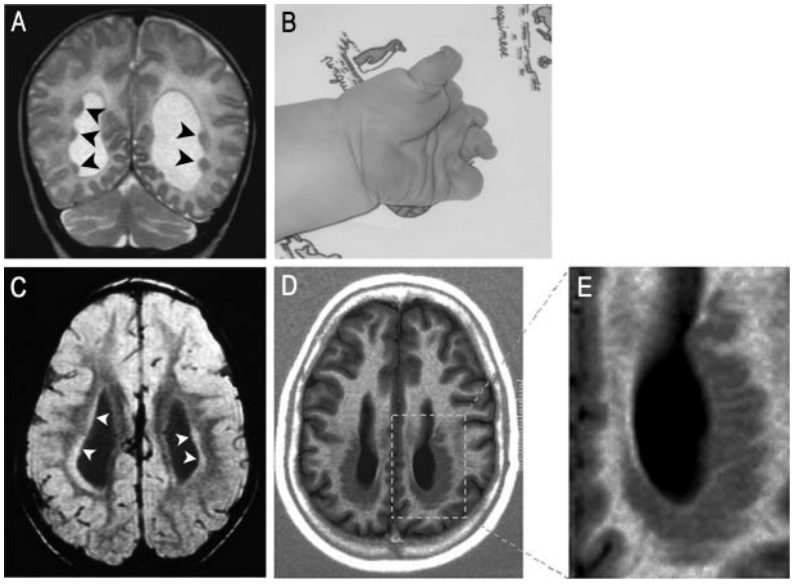

Fig. 4 **A** and **B** illustrate PNH and severe limb limb reduction abnormality in a 2-year-old girl. In **A**, a coronal section shows non-contiguous heterotopic nodules (arrowheads) and dilated ventricles. In **B**, the left hand is shown. In **C**, an axial section in a 15-year-old girl with diffuse linear PH surrounding the lateral ventricles (arrowheads); no nodules can be seen. There is thickening of the cortex with simplified gyral pattern especially in the frontal lobes. **D** and **E** show PH with ribbon-like aspect in a 25 years old woman. **D** is an axial section showing grey matter heterotopia surrounding the posterior aspect of the lateral ventricles and **E** is a magnification showing the nearly sinusoidal ribbon like structure of the heterotopic grey matter that is reminiscent of a simplified gyral pattern.

or fingers and of metatarsal or metacarpal bones (Fig. 4B). These four patients had mild mental retardation and one had epilepsy. Mutation analysis of *FLNA*, performed in two, was negative. Two boys had the bilateral PNH, mental retardation–syndactyly syndrome (patients BPNH-03 and BPNH-12 in Dobyns *et al.*, 1997). Mutation analysis of *FLNA*, performed in both, was negative. In previous studies, a large duplication of Xq28 also containing *FLNA*, had been demonstrated in a third boy with an identical phenotype, not included in this series (patient BPNH-02 in Dobyns *et al.*, 1997 also reported by Fink *et al.*, 1997 and Fox *et al.*, 1998). The same duplication was not identified in the two patients reported here (Fink *et al.*, 1997), prompting us to perform mutation analysis. Further studies at the molecular karyotyping and intragenic level are in progress in these two patients in order to identify deletions or duplications of *FLNA*.

Bilateral PNH with Ehlers–Danlos syndrome

Three unrelated women had classical bilateral PNH associated with EDS (Fig. 1C and D). Two of them had epilepsy; one had borderline cognitive level and the remaining two had normal intelligence. Two of them were described in a previous report (Sheen *et al.*, 2005; patients F7 and F8), while the third patient (5-II.1) is reported in detail below (*see* Family 5). Mutation analysis of *FLNA* revealed a single base deletion in two probands and a missense mutation in one.

Bilateral PNH with fragile-X syndrome

Two boys with the fragile-X syndrome (age 13 years and 4 years) were found to have PNH on brain imaging. One of them had small scattered bilateral subependymal nodules as well as malrotated hippocampi; the second had a single large nodule beneath the right lateral ventricle. Neither of them had epilepsy. Southern blotting demonstrated a CGG trinucleotide repeat expansion in the 5′ end of the *Fragile site mental retardation 1* (*FMR1*) gene in both boys.

Other syndromes with bilateral PNH

Two additional syndromes with bilateral PNH were less clearly characterized and seen in a few patients. Two boys had bilateral periventricular micronodular heterotopia, with scattered subependymal nodules, each less than a few millimetres thick. These nodules barely altered the ventricular profile and could only be seen on high resolution MRI, which was prompted by childhood onset seizures and mental retardation in both patients. One additional individual with ambiguous genitalia was born with pseudohermaphroditism, characterized by intra-abdominal testes, penoscrotal hypospadia with adjacent uterine tubes and vagina. An orchiectomy was performed and female hormonal therapy given, and the child was raised as a girl. Her cognitive level was normal. Standard karyotype was 46,XY and FISH (fluorescent *in situ* hybridization) for subtelomeric imbalances was negative. After onset of generalized seizures at 25 years, brain MRI revealed bilateral PNH. Mutation analysis of *FLNA* was negative in all three patients.

Unilateral diffuse PNH sparing the temporal horns

Fifteen patients (7 male; 8 female; age 3–36 years, mean age: 17 years) had unilateral PNH whose characteristics were similar to those of classical bilateral PNH, although lateralized (Fig. 1B). No associated brain or extracerebral malformations were seen. Thirteen patients were sporadic with no reported consanguinity; mutation analysis was negative in 8 of these patients. In one family, a father and daughter had unilateral PNH on opposite sides (Guerrini *et al.*, 2004; patients 2-II.3 and 2-III.1). Mutation analysis of *FLNA* demonstrated an S149P mutation in both individuals, as well as in the asymptomatic proband's paternal grandmother who refused brain MRI scanning. The S149P change must therefore be germline at least in the two individuals who inherited it (i.e. somatic mosaicism cannot account for the unilateral presentation). Among the entire group, eight patients had epilepsy; one had had infantile spasms and all the remaining had focal epilepsy. Age at seizure onset ranged from 1 to 38 years (mean 16 years). Seven patients had normal cognitive level and eight had mild mental retardation.

Diffuse linear PH

Three unrelated children, two boys and a girl, had PH characterized by a smooth layer of subependymal grey matter rather than discrete or confluent nodules (Fig. 4C). The gyral pattern was mildly simplified with areas of infolding and abnormally thick cortex suggestive of a widespread malformation of neuronal migration. All three children had severe developmental delay, mental retardation and epilepsy. Mutation analysis of *FLNA*, performed in all, gave negative results.

PH with ribbon-like aspect

Two unrelated patients, a man and a woman in their early adulthood, had ribbon-like PH encircling the posterior bodies and occipital horns of the lateral ventricles. On close inspection, the heterotopic ribbon appeared convoluted with a nearly sinusoidal regularity reminiscent of a simplified gyral pattern (Fig. 4D and E). There were no associated malformations. Both patients presented with childhood onset seizures that prompted brain imaging studies, and had normal intelligence; both were sporadic. Mutation analysis of *FLNA* was not performed. Mutation analysis of the doublecortin (*DCX*) gene in one patient gave negative results.

FLNA mutations

We found 25 mutations of the *FLNA* gene in 40 patients, including 16 novel mutations. The latter consisted of 4 splice site mutations, 5 nonsense mutations, 5 deletions and 2 insertions (Table 2, Fig. 6).

Twenty-five patients belonged to 10 families with X-linked PNH and mutations were found in all of them (100%). Four families with classical bilateral PNH (Family 1 and 2 in Moro *et al.*, 2002; Family 1 and 4 in Guerrini *et al.*, 2004) and one family with unilateral PNH (Family 2 in Guerrini *et al.*, 2004) were described in previous reports. Five unreported families, including four with classical bilateral PNH and one with EDS in the proband, are described in the following section. Fifteen patients were sporadic: 13 had classical bilateral PNH (including Patient 1-II.2 of Parrini *et al.*, 2004) and 2 had associated EDS (including Patients F7 and F8 of Sheen *et al.*, 2005).

Overall, the rate of *FLNA* mutations was 49% in patients with classical bilateral PNH, of which 33 were in 43 females (77%) and 2 in 29 males (7%), irrespective of their being familial or sporadic, but ranged from 100% in familial cases (3 males, 19 females) to 26% in sporadic patients (13 out of 50 patients). In particular, the probability of finding *FLNA* mutations in a sporadic individual with classical bilateral PNH was 54% in females (13 out of 24) and 0% in males (0 out of 26); while in individuals with other phenotypes it was 8% (2 out of 24) in females and 0% (0 out of 24) in males, limited to the 2 minor variants of EDS and unilateral PNH. Thirty-seven out of 40 patients (93%) with mutations of *FLNA* were female.

Novel mutations

Familial cases

Family 1 (Table 2; individuals 2a and b): The proband (Fig. 5, 1-II.3) was a 20-year-old woman with borderline intelligence quotient (IQ) [Full Scale Intelligence Quotient (FSIQ) = 69] and headache, who had an MRI scan following episodes of delirium that were interpreted as of psychotic origin. Her brain MRI and that of her 24-year-old sister (Fig. 5, 1-II.4) revealed classical bilateral PNH. DHPLC analysis of *FLNA* showed an abnormal elution profile for exon 31, and sequencing revealed a c.5327 C→T nucleotide substitution. The latter causes a G1710G silent mutation that was predicted to be recognized as an alternative splice acceptor site (BDGP splice database score = 0.99). To verify the hypothesis of alternative splicing, a fragment spanning 700 bp of *FLNA* cDNA encompassing the mutation site (from exon 31 to 32) was amplified from cDNA obtained by RT–PCR from patient-derived lymphoblastoid cells, and subsequently sequenced. The resulting cDNA sequence (exons 31–32) was normal and did not show the nucleotide variation identified in genomic DNA, suggesting that the allele carrying the mutation was not correctly expressed. Subcloned RT–PCR products showed that 1 out of 39 clones contained a shorter aberrant mRNA spliced insert (352 bp instead of 412 bp) with a new donor splice site created by the c.5327 C→T nucleotide substitution. Both NMD and skewed X-chromosome inactivation might explain the underexpression of the mutated allele. NMD is an RNA surveillance mechanism essential for maintaining mRNA quality control by degrading mRNAs containing premature termination codons (Holbrook *et al.*, 2004). The RT–PCR,

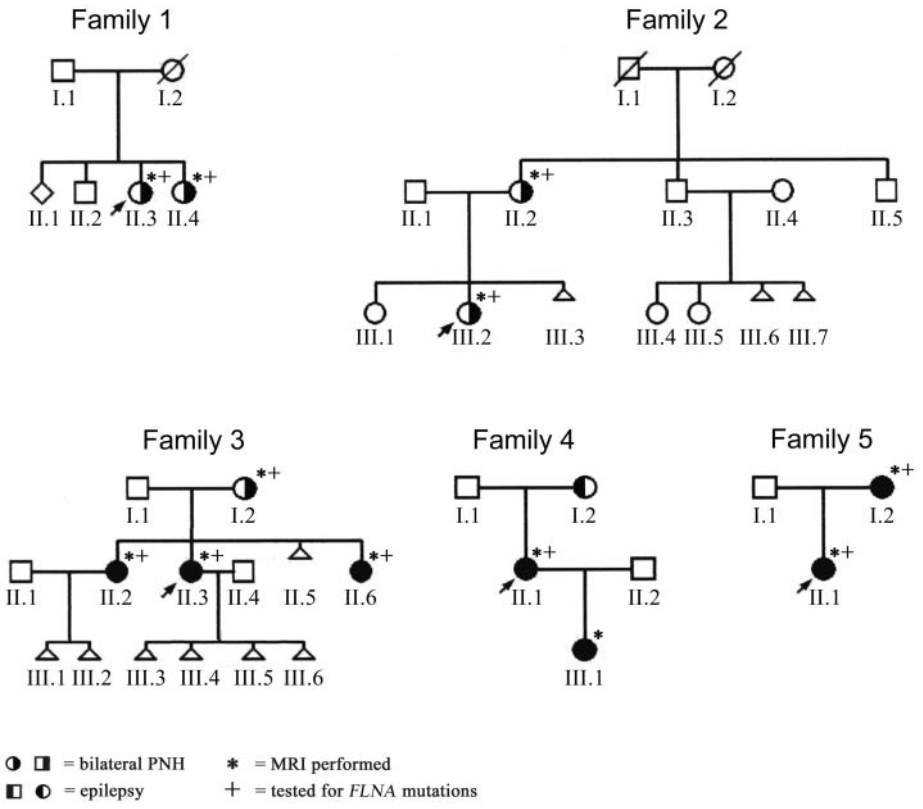

Fig. 5 Pedigrees of families 1–5.

subcloning and sequence analysis performed on the patient's lymphoblastoid cell line treated with cycloheximide showed an increased number of clones (8 out of 35) containing the aberrant mRNA splicing product, consistent with NMD (Fig. A in the Supplementary online material). In addition, X-inactivation studies in the patient's lymphoblastoid cell line revealed a significant skewing with an 80 : 20 ratio (data not shown). These results indicate that both NMD and skewed X-chromosome inactivation have contributed to the prevalent expression of the normal allele in the patient's lymphoblastoid cell line.

Family 2 (Table 2; individuals 6a and b): The proband (Fig. 5; 2-III.2) was a 15-year-old girl with idiopathic thrombocytopenia, PDA, severe scoliosis, joint laxity and dental malposition. Brain MRI (Fig. 1A) revealed classical bilateral PNH in the proband and in her mother (Fig. 5; 2-II.2). DHPLC analysis showed an abnormal profile of exon 13 of the *FLNA* gene in the proband; sequencing analysis revealed a c.2002 C→T nucleotide substitution in both patients, leading to a protein truncation (Q668X).

Family 3 (Table 2; individuals 7a–d): The proband (Fig. 5; 3-II.3) was a 33-year-old woman with classical bilateral PNH and epilepsy who had had four miscarriages. Both patients' sisters (Fig. 5; 3-II.2 and 3-II.6) had classical bilateral PNH and epilepsy; their mother (Fig. 5; 3-I.2) had classical bilateral PNH but no epilepsy. DHPLC analysis in the proband showed an abnormal profile of exon 25. Sequencing revealed a substitution of 2 nt (c.[4437 A→G;4438 C→A]) in all affected individuals, thus suggesting that the change was in a *cis* configuration, leading to a TGA stop codon (Y1479X). We confirmed the *cis* configuration subcloning the PCR product of exon 25 in Patient 6a (Fig. B in the Supplementary online material).

Family 4 (Table 2; individual 9a): The proband (Fig. 5; 4-II.1) was a 49-year-old woman with classical bilateral PNH and epilepsy. Her 5-year-old daughter was also affected and her mother was also probably affected as she had epilepsy but refused MRI scan of the brain and DNA analysis. All three individuals had normal intelligence. DHPLC analysis in the proband showed an abnormal chromatographic profile of exon 41. Sequencing detected a c.6724 C→T change, resulting in a stop codon and truncation of the protein at position 2242 (R2242X).

Sporadic patients

Eleven novel *FLNA* mutations were found in many sporadic women with classical bilateral PNH (Table 2 and Fig. 6). We found splice site mutations in three patients, truncating mutations in two, deletions in four and insertions in two.

FLNA mutations in Ehlers–Danlos syndrome

The mutations associated with bilateral PNH and EDS in two sporadic patients included in this series were previously

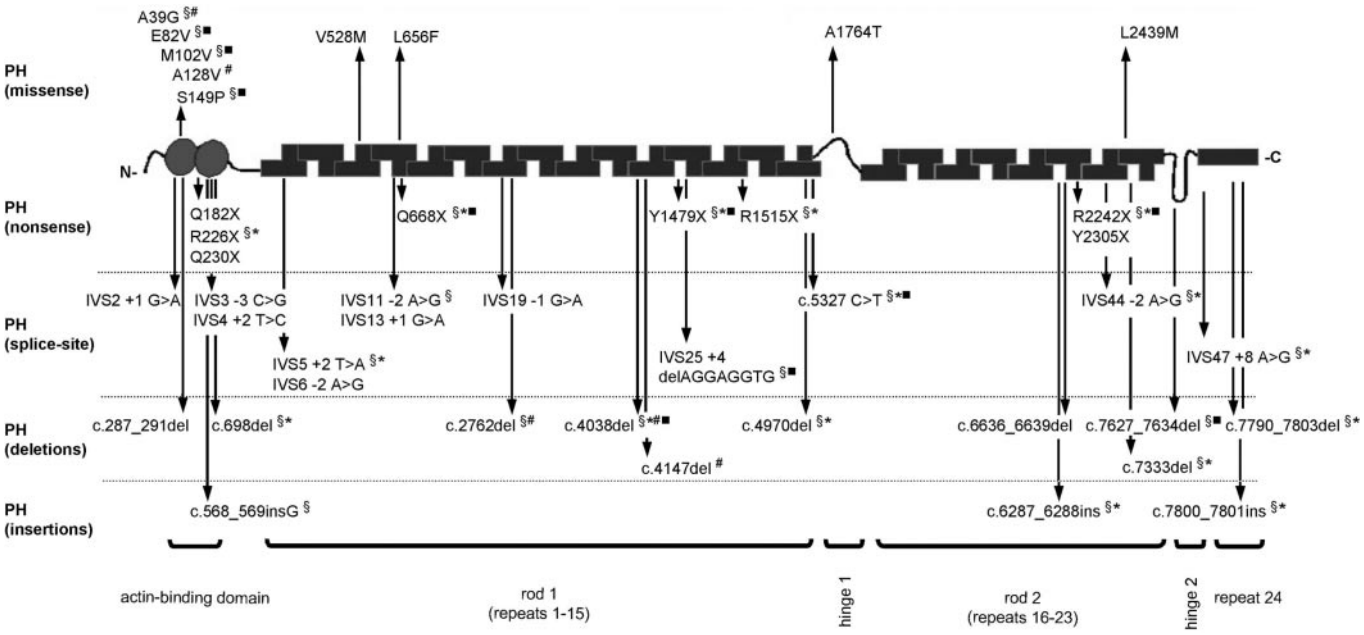

Fig. 6 Location of *FLNA* mutations (see Table 2 and Table A in Supplementary online material) on the structure of the FLNA monomer containing repeat blocks of 96 amino acids (Gorlin *et al.*, 1990). In the upper part of the panel are shown *FLNA* missense mutations associated with periventricular heterotopia (PH). In the bottom part of the panel are shown *FLNA* mutations causing frame-shift or protein truncation (nonsense, splice-site, deletions and insertions) that are associated with PH. §Known *FLNA* mutations also observed in this study; *new *FLNA* mutations reported in this study; familial cases in this study; #EDS associated mutations.

reported (c.2762 delG in exon 19 and A39G in exon 2; Sheen *et al.*, 2005), but we have new data on an additional patient.

Family 5 (Table 2; individuals 11a and b): The proband (Fig. 5; 5-II.1) had bilateral PNH associated with EDS and epilepsy, with joint hypermobility, soft hyperelastic skin with widened paper-thin scars, dysmorphic facial features with hypertelorism, hypoplastic midface, short nose, long shallow philtrum, cupid's bow upper lip and micrognathia. Her intelligence was normal. Her mother (Fig. 5; 5-I.2) also had epilepsy and bilateral PNH (Fig. 1C), but no dysmorphic features or signs of EDS. DHPLC showed an abnormal profile of exon 24 in the proband and sequencing revealed a c.4038 delG in both patients, resulting in a frameshift and presumed protein truncation.

Statistical analysis

Combining our results with previously reported mutations of *FLNA* in patients with PNH, we found 14 mutations in the ABD (904 nt; 10.2% of the gene), 17 in the Rod 1 + Hinge 1 domain (5029 nt; 56.7% of the gene), 8 in the Rod 2 + Hinge 2 domain (2629 nt; 29.7% of the gene), and 3 in the C-terminal domain (299 nt; 3.4% of the gene). Statistical analysis using Fisher's exact test indicated that the number of *FLNA* mutations was significantly different in the ABD ($P = 0.0087$) compared to the number occurring in the three remaining domains. Therefore, the ABD is a hotspot for mutations causing bilateral PNH. No significant association was found for the Rod 1 + Hinge 1, Rod 2 + Hinge 2 or C-terminal domains ($P > 0.05$ for all three).

The χ^2 test indicated that the sex ratio in the 37 patients with classical bilateral PNH without *FLNA* mutations was significantly skewed towards males (26 males and 11 females: $P = 0.013$).

Discussion

The main aim of our analysis was to offer new insights into the nosology of PH, for optimizing genetic counselling and future research. Our study examined the clinical and brain MRI characteristics of 182 individuals with PH, including bilateral PNH and other types of PH and led to the definition of 15 distinct malformation patterns (Table 1). The overall information that can be drawn from this study is that PH is an extremely heterogeneous disorder regarding both clinical and brain imaging presentation and genetic causes. Classical bilateral PNH represented the largest group (98 patients: 54%). In most of the 15 additional phenotypes (84 patients: 46%), PH was associated with other brain malformations, including hippocampal malformation and cerebellar hypoplasia, bilateral fronto-perisylvian or temporo-parieto-occipital PMG, hydrocephalus and microcephaly. However, it was possible to identify a smaller group of patients in whom PH was associated with non-neurologial defects including EDS, frontonasal dysplasia, limb abnormalities, ambiguous genitalia and fragile-X syndrome. Finally, several distinct subgroups of patients were identified in whom the PH presented an unusual appearance,

including: micronodular appearance, unilateral distribution and laminar or ribbon-like shapes.

Phenotypes associated with *FLNA* mutations

FLNA appears to be the major gene associated with PH. In this study, *FLNA* mutations were associated with the most common phenotype, classical bilateral PNH, and with two minor variants: unilateral PNH and bilateral PNH with EDS. *FLNA* maps to Xq28 and codes for the high molecular mass protein filamin A which mediates crucial processes for spatial and temporal coordination of cell reshaping and motility. Although X-linked and sporadic PNH has been associated with *FLNA* mutations (Fox *et al.*, 1998), PH is expected to be genetically heterogeneous. For instance, recessive PH with microcephaly has been associated with *ARFGEF2* mutations (Sheen *et al.*, 2003*a*; Sheen *et al.*, 2004*a*).

Mutation analysis of *FLNA* in a cohort of 120 probands from our total group of 182 with PH (~50% males and ~50% females) uncovered 25 *FLNA* mutations of which 16 are novel. Consistent with prior reports, the sex ratio among these patients is skewed toward females: 93% of patients harbouring *FLNA* mutations were female and 7% were males. Mutations of *FLNA* were found in all familial cases of classical X-linked bilateral PNH (8 families; 22 affected individuals) as previously reported (Sheen *et al.*, 2004*a*), while about 26% of sporadic patients, all females, with classical bilateral PNH harbour an *FLNA* mutation. Overall, the probability of identifying a mutation in an individual with classical bilateral PNH was 49%, but this decreased to 4% in patients with other phenotypes, irrespective of their being familial or sporadic. We identified additional *FLNA* mutations only in patients with unilateral PH and with bilateral PNH associated with EDS. Thus, the cause of the PH remained unknown in 51% of patients with classical bilateral PNH, and in 96% of those with other PH phenotypes, confirming causal heterogeneity of PH. We believe that all or most of the remaining causes are genetic based on reports of other loci (dup 5p15.1 and dup 5p15.33) and genes (*ARFGEF2*), skewing of the sex ratio in at least two syndromes, and lack of evidence supporting extrinsic causes (Sheen *et al.*, 2003*b*; Sheen *et al.*, 2004*a*; Wieck *et al.*, 2005).

A family with unilateral PH and a missense mutation (S149P) had already been reported (Family 2 in Guerrini *et al.*, 2004). In this family, we hypothesized the mild male phenotype and father to daughter transmission to be consistent with mild functional impairment of the FLNA protein.

A previous description of PNH with EDS (Sheen *et al.*, 2005) included the missense mutation and truncating mutation in the two patients also described here (Patients F7 and F8 in Sheen *et al.*, 2005). In the present study, we have also identified an *FLNA* deletion (c.4038 delG) in a family (Family 5) in which the proband (5-II.2) had PNH with EDS but her mother (5-I.2) had only classical bilateral PNH, suggesting that the clinical features of EDS may reflect variable expressivity, most likely due to genetic modifying factors. Phenotypic heterogeneity might also result from skewed X-inactivation in either woman or somatic mosaicism in the mother. The association between PNH and EDS changes the understanding of the molecular pathogenesis of EDS. Generally, different types of EDS have been associated with alterations of the cross-linkage and adhesion of collagen fibrils in the extracellular matrix (Sheen *et al.*, 2005). FLNA has been shown to bind beta integrin cell adhesion receptors and this interaction is possibly involved in cell migration (Sharma *et al.*, 1995; Calderwood *et al.*, 2001). Impaired cellular adhesion due to *FLNA* mutations might therefore be responsible for both the defects in connective tissue seen in EDS and failure in neuronal migration from the ventricular zone, which is typical of PNH. Overall, only 3 out of the 40 patients (7.5 %) reported here with PNH and an *FLNA* mutation also had EDS. Mutations identified in these patients did not cluster in any specific *FLNA* region and were predicted to cause variable functional consequences in the protein product. In addition, in most patients with the PNH-EDS phenotype no *FLNA* mutations can be demonstrated (Sheen *et al.*, 2005). These observations leave the genetic basis of the PNH-EDS phenotype unexplained.

This study brings to 42 the number of mutations of *FLNA* so far described in association with PNH, with or without EDS (Fig. 6). Considering all 42 *FLNA* mutations identified (Fig. 6), the prevalence of mutations in the ABD was significantly elevated (14 out of 42 in 904 nt) ($P < 0.05$) compared with the prevalence of mutations in the other three domains (28 out of 42 in 7957 nt) ($P > 0.05$). This result suggests that the ABD is a hotspot for *FLNA* mutations causing PNH. Therefore, mutation analysis of exons encompassing the ABD should be performed first in these patients.

Some regions of *FLNA* have been identified that are associated with other specific disorders. Missense mutations falling within the CH2 domain and rod-domain repeats 3, 10 or 14/15 were observed in males with OPD1 or OPD2 (Robertson *et al.*, 2003). However, no mutations leading to OPD1 or OPD2 fell within the CH1 domain. All four missense mutations we found fell within the CH1 domain and none in the CH2 domain. Overall, no missense mutations in CH2 have been identified in patients with PNH (Fig. 6) but several early truncating mutations causing loss of the CH2 domain have been detected in patients with PNH without the OPD phenotype. This observation confirms previous suggestions that missense mutations in CH1 in patients with PNH cause loss of function, while missense mutations in CH2, which are always associated with the OPD spectrum, cause a gain of function (Sheen *et al.*, 2001; Robertson *et al.*, 2003).

Overall, only 9 of the 42 *FLNA* mutations that have so far been associated with PNH are missense mutations, suggesting that mutations causing protein truncation are the main cause of the PNH phenotype. This contrasts sharply with the

OPD syndromes that have been associated only with missense mutations (Robertson *et al.*, 2003). This observation confirms that distinct pathogenic mechanisms underlie these two different phenotypes.

In general, some correlation between the severity of *FLNA* mutations and the associated PNH phenotype seems to exist but is not yet clear even with this large number of mutations. In our study we did not observe significant differences between the type and location of mutations, and the severity of the associated phenotype. One exception is represented by missense germline mutations and distal truncating mutations that are compatible with survival of affected males, while insertions, deletions or truncating mutations are lethal in males. Partial or residual function of the protein presumably accounts for male viability (Sheen *et al.*, 2001; Guerrini *et al.*, 2004). Somatic mosaicism in patients with truncating mutations may also attenuate the phenotype (Guerrini *et al.*, 2004; Parrini *et al.*, 2004).

Classical bilateral PNH not associated with *FLNA* mutations

Classical bilateral PNH was observed in 37 (51%) of the patients in whom *FLNA* mutations were not found. These patients did not show significant clinical and imaging differences with respect to those with mutations. Mutations in non-coding regions, larger deletions/duplications involving one or more exons, and cryptic chromosomal abnormalities involving *FLNA* may still account for some of the patients in whom no mutations were detected. However, sex ratio in this group reached statistical significance towards male predominance ($P = 0.013$), suggesting that an alternative X-linked recessive gene may play a major role. However, some ascertainment bias due to a higher proportion of males being referred due to their more severe phenotype cannot be excluded.

Major phenotypes not associated with *FLNA* mutations

None of the patients belonging to these groups harboured mutations in *FLNA,* suggesting that other genes are likely to play a major role. However, *FLNA* cannot be completely ruled out as the disease gene as mutations in non-coding regions, larger deletions/duplications involving one or more exons, and cryptic chromosomal abnormalities involving *FLNA* might still be responsible for these phenotypes. Amongst patients with bilateral PNH associated with non-neurological defects, at least four groups were homogeneous and large enough to be considered as new syndromes or to confirm previously hypothesized syndromes. Patients with bilateral frontal-perisylvian PNH-PMG, bilateral posterior PNH-PMG, and those with autosomal recessive bilateral PNH and microcephaly have been the subject of separate reports and will not be discussed further here (Sheen *et al.*, 2004*a*; Wieck *et al.*, 2005). Another syndrome consisting of severe congenital microcephaly, diffuse PNH and diffuse PMG was reported in two patients (Wieck *et al.*, 2005), but not seen in this series.

Bilateral posterior PNH with hippocampal malformation and cerebellar hypoplasia represents a newly recognized syndrome found in more females than males, but without significant skewing of the sex ratio in this first small group of ten patients. It must be differentiated from classical bilateral PNH due to *FLNA* mutations. The main difference is in the location of the heterotopic nodules, which in classical bilateral PNH are diffuse but do not extend into the temporal horns and do not usually surround the hippocampal formation. Incomplete hippocampal rotation is often observed in patients with neuronal migration disorders (Baulac *et al.*, 1998) but may also occur as an isolated abnormality (Fernandez *et al.*, 1998). In the patients described here, malrotated hipocampi are associated with abnormal neuronal migration in the parahippocampal cortex and in mesial temporal structures. Patients in this group had severely hypoplastic cerebellum. Vermis hypoplasia with mega cisterna magna is also present in some patients with classical bilateral PNH due to *FLNA* mutations (Fox *et al.*, 1998) but is never as severe as in the patients reported here, for most of whom cerebellar signs prompted neuroradiological investigations. Cognitive level and types of epilepsy did not differ from what is usually observed in classical bilateral PNH.

Bilateral posterior PNH with hydrocephalus was observed in seven patients, most having severe developmental delay and epilepsy. The sex ratio in this group was balanced suggesting an autosomal pattern of inheritance. Sheen *et al.* (2004*b*) reported weakly positive linkage to Xq28 in one family, but no mutations were found in *FLNA* or in *L1CAM (L1 cell adhesion molecule)*, a gene associated with hydrocephalus, Hirschsprung disease and agenesis of the corpus callosum. While the PNH-hydrocephalus phenotype is quite homogeneous, its genetic basis is probably heterogeneous.

Bilateral PNH with frontonasal dysplasia was observed in six sporadic boys and one girl. Mild mental retardation was present in all and epilepsy in three. Two of the boys had been previously described (Guerrini and Dobyns, 1998). The five additional patients included in the present study confirm the specificity of the syndrome and bring to six males and two females (seven cases included herein and one girl reported by Guion-Almeida and Richieri-Costa, 1999) the total number of patients described so far. Skewing of gender ratio does not reach statistical significance (Fisher's exact test: $P > 0.05$).

Bilateral PNH with limb abnormalities was observed in six patients; all had mental retardation and two had epilepsy. Severity of limb abnormalities was variable, ranging from severe limb reduction with missing or hypoplastic phalanges of fingers and toes to syndactyly. All patients were sporadic and gender ratio in this group was balanced. Recessive or '*de novo*' dominant mutations are both possible. Genes regulating limb development are possible candidates for this syndrome. In particular *FGF8*, involved in the FGF (fibroblast growth factor) signalling from the apical ectodermal

ridge (Lewandoski *et al.*, 2000), could be a good candidate as there is evidence that it is involved in neocortical patterning (Fukuchi-Shimogori and Grove, 2003).

Minor phenotypes with PH

We identified five additional rare conditions with PH. No mutations of *FLNA* were identified in these small subgroups of patients but not all of them were tested. These observations confirm the phenotypic and genotypic diversity associated with PH.

Fragile-X syndrome had been diagnosed in two boys with isolated or scattered PH and a full mutation of *FMR1*, suggesting a possible role of this gene in neuronal migration. Bilateral periventricular micronodular heterotopia and bilateral PNH with ambiguous genitalia were observed in three patients only and are less clearly characterized.

Diffuse linear PH occurred in association with more widespread cortical thickening suggesting a generalized migration abnormality differently affecting migrating and non-migrating neurons. PH with ribbon-like shape occurred as an isolated abnormality affecting a subset of abnormally migrating neurons that although receiving the genetic information to assemble in a convoluted, cortical-like pattern, were not able to reach their final destination.

Supplementary material

The Supplementary data are available at *Brain* on-line.

Acknowledgements

We thank the patients, their families, and the referring physicians. C.A.W. is an Investigator of the Howard Hughes Medical Institute. This study complies with the current Italian laws and was supported with funding from Fondazione Pierfranco e Luisa Mariani (grant R-04-35), the Italian Ministry of Health (grant RF 2/02) and grants from the NINDS (R37 NS35129) to C.A.W.

References

Allen RC, Zoghbi HY, Moseley AB, Rosenblatt HM, Belmont JW. Methylation of HpaII and HhaI sites near the polymorphic CAG repeat in the human androgen-receptor gene correlates with X chromosome inactivation. Am J Hum Genet 1992; 51: 1229–39.

Baulac M, De Grissac N, Hasboun D, Oppenheim C, Adam C, Arzimanoglou A, et al. Hippocampal developmental changes in patients with partial epilepsy: magnetic resonance imaging and clinical aspects. Ann Neurol 1998; 44: 223–33.

Barkovich AJ, Kjos BO. Gray matter heterotopias: MR characteristics and correlation with developmental and neurologic manifestations. Radiology 1992; 182: 493–9.

Calderwood DA, Huttenlocher A, Kiosses WB, Rose DM, Woodside DG, Schwartz MA, et al. Increased filamin binding to beta-integrin cytoplasmic domains inhibits cell migration. Nat Cell Biol 2001; 3: 1060–8.

Carroll RC, Gerrard JM. Phosphorylation of platelet actin-binding protein during platelet activation. Blood 1982; 59: 466–71.

Chen M, Stracher A. In situ phosphorylation of platelet actin-binding protein by cAMP-dependent protein kinase stabilizes it against proteolysis by calpain. J Biol Chem 1989; 264: 14282–9.

Cunningham CC. Actin polymerization and intracellular solvent flow in cell surface blebbing. J Cell Biol 1995; 129: 1589–99.

Dobyns WB, Andermann E, Andermann F, Czapansky-Beilman D, Dubeau F, Dulac O, et al. X-linked malformations of neuronal migration. Neurology 1996; 47: 331–9.

Dobyns WB, Guerrini R, Czapansky-Beilman DK, Pierpont ME, Breningstall G, Yock DH Jr, et al. Bilateral periventricular nodular heterotopia with mental retardation and syndactyly in boys: a new X-linked mental retardation syndrome. Neurology 1997; 49: 1042–7.

Dulabon L, Olson EC, Taglienti MG, Eisenhuth S, McGrath B, Walsh CA, et al. Reelin binds alpha3beta1 integrin and inhibits neuronal migration. Neuron 2000; 27: 33–44.

Eksioglu YZ, Scheffer IE, Cardenas P, Knoll J, DiMario F, Ramsby G, et al. Periventricular heterotopia: an X-linked dominant epilepsy locus causing aberrant cerebral cortical development. Neuron 1996; 16: 77–87.

Fernandez G, Effenberger O, Vinz B, Steinlein O, Elger CE, Dohring W, et al. Hippocampal malformation as a cause of familial febrile convulsions and subsequent hippocampal sclerosis. Neurology 1998; 50: 909–17.

Fink JM, Dobyns WB, Guerrini R, Hirsch BA. Identification of a duplication of Xq28 associated with bilateral periventricular nodular heterotopia. Am J Hum Genet 1997; 61: 379–87.

Fox JW, Lamperti ED, Eksioglu YZ, Hong SE, Feng Y, Graham DA, et al. Mutations in filamin 1 prevent migration of cerebral cortical neurons in human periventricular heterotopia. Neuron 1998; 21: 1315–25.

Fukuchi-Shimogori T, Grove EA. Emx2 patterns the neocortex by regulating FGF positional signalling. Nat Neurosci 2003; 6: 825–31.

Gorlin JB, Yamin R, Egan S, Stewart M, Stossel TP, Kwiatkowski DJ, et al. Human endothelial actin-binding protein (ABP-280, non-muscle filamin): a molecular leaf spring. J Cell Biol 1990; 111: 1089–105.

Guion-Almeida ML, Richieri-Costa A. Frontonasal dysplasia, macrobleopharon, eyelid colobomas, ear anomalies, macrostomia, mental retardation and CNS structural anomalies. A new syndrome? Clin Dysmorphol 1999; 8: 1–4.

Guerrini R, Dobyns WB. Bilateral periventricular nodular heterotopia with mental retardation and frontonasal malformation. Neurology 1998; 51: 499–503.

Guerrini R, Carrozzo R. Epilepsy and genetic malformations of the cerebral cortex. Am J Med Genet 2001; 106: 160–73.

Guerrini R, Mei D, Sisodiya S, Sicca F, Harding B, Takahashi Y, et al. Germline and mosaic mutations of FLN1 in men with periventricular heterotopia. Neurology 2004; 63: 51–6.

Hidalgo-Bravo A, Pompa-Mera EN, Kofman-Alfaro S, Gonzalez-Bonilla CR, Zenteno JC. A novel filamin A D203Y mutation in a female patient with otopalatodigital type 1 syndrome and extremely skewed X chromosome inactivation. Am J Med Genet A 2005; 136: 190–3.

Himmel M, Van Der Ven PF, Stocklein W, Furst DO. The limits of promiscuity: isoform-specific dimerization of filamins. Biochemistry 2003; 42: 430–9.

Hock RS, Davis G, Speicher DW. Purification of human smooth muscle filamin-and characterization of structural domains and functional sites. Biochemistry 1990; 29: 9441–51.

Holbrook JA, Neu-Yilik G, Hentze MW, Kulozik AE. Nonsense-mediated decay approaches the clinic. Nat Genet 2004; 36: 801–8.

Huttenlocher PR, Taravath S, Mojtahedi S. Periventricular heterotopia and epilepsy. Neurology 1994; 44: 51–5.

Lewandoski M, Sun X, Martin GR. Fgf8 signalling from the AER is essential for normal limb development. Nat Genet 2000; 26: 460–3.

Loo DT, Kanner SB, Aruffo A. Filamin binds to the cytoplasmic domain of the beta1-integrin. Identification of amino acids responsible for this interaction. J Biol Chem 1998; 273: 23304–12.

Meyer SC, Zuerbig S, Cunningham CC, Hartwig JH, Bissell T, Gardner K, et al. Identification of the region in actin-binding protein that binds to the cytoplasmic domain of glycoprotein IBalpha. J Biol Chem 1997; 272: 2914–19.

Moro F, Carrozzo R, Veggiotti P, Tortorella G, Toniolo D, Volzone A, et al. Familial periventricular heterotopia: missense and distal truncating mutations of the FLN1 gene. Neurology 2002; 58: 916–21.

Noegel AA, Leiting B, Witke W, Gurniak C, Harloff C, Hartmann H, et al. Biological roles of actin-binding proteins in Dictyostelium discoideum examined using genetic techniques. Cell Motil Cytoskeleton 1989; 14: 69–74.

Ott I, Fischer EG, Miyagi Y, Mueller BM, Ruf W. A role for tissue factor in cell adhesion, migration mediated by interaction with actin-binding protein 280. J Cell Biol 1998; 140: 1241–53.

Palm L, Hagerstrand I, Kristoffersson U, Blennow G, Brun A, Jorgensen C. Nephrosis and disturbances of neuronal migration in male siblings—a new hereditary disorder? Arch Dis Child 1986; 61: 545–8.

Parrini E, Mei D, Wright M, Dorn T, Guerrini R. Mosaic mutations of the FLN1 gene cause a mild phenotype in patients with periventricular heterotopia. Neurogenetics 2004; 5: 191–6.

Robertson SP, Twigg SR, Sutherland-Smith AJ, Biancalana V, Gorlin RJ, Horn D, et al. Localized mutations in the gene encoding the cytoskeletal protein filamin-a cause diverse malformations in humans. Nat Genet 2003; 33: 487–91.

Sharma CP, Ezzell RM, Arnaout MA. Direct interaction of filamin (ABP-280) with the beta 2-integrin subunit CD18. J Immunol 1995; 154: 3461–70.

Sheen VL, Dixon PH, Fox JW, Hong SE, Kinton L, Sisodiya SM, et al. Mutations in the X-linked filamin 1 gene cause periventricular nodular heterotopia in males as well as in females. Hum Mol Genet 2001; 10: 1775–83.

Sheen VL, Feng Y, Graham D, Takafuta T, Shapiro SS, Walsh CA. Filamin-a and Filamin-b are co-expressed within neurons during periods of neuronal migration and can physically interact. Hum Mol Genet 2002; 11: 2845–54.

Sheen VL, Topcu M, Berkovic S, Yalnizoglu D, Blatt I, Bodell A, et al. Autosomal recessive form of periventricular heterotopia. Neurology 2003a; 60: 1108–12.

Sheen VL, Wheless JW, Bodell A, Braverman E, Cotter PD, Rauen KA, et al. Periventricular heterotopia associated with chromosome 5p anomalies. Neurology 2003b; 60: 1033–66.

Sheen VL, Ganesh VS, Topcu M, Sebire G, Bodell A, Hill RS, et al. Mutations in ARFGEF2 implicate vesicle trafficking in neural progenitor proliferation and migration in the human cerebral cortex. Nat Genet 2004a; 36: 69–76.

Sheen VL, Basel-Vanagaite L, Goodman JR, Scheffer IE, Bodell A, Ganesh VS, et al. Etiological heterogeneity of familial periventricular heterotopia and hydrocephalus. Brain Dev 2004b; 26: 326–34.

Sheen VL, Jansen A, Chen MH, Parrini E, Morgan T, Ravenscroft R, et al. Filamin-a mutations cause periventricular heterotopia with Ehlers-Danlos syndrome. Neurology 2005; 64: 254–62.

Stefanova M, Meinecke P, Gal A, Bolz H. A novel 9 bp deletion in the filamin-a gene causes an otopalatodigital-spectrum disorder with a variable, intermediate phenotype. Am J Med Genet A 2005; 132: 386–90.

Stendahl OI, Hartwig JH, Brotschi EA, Stossel TP. Distribution of actin-binding protein and myosin in macrophages during spreading and phagocytosis. J Cell Biol 1980; 84: 215–24.

Stossel TP, Condeelis J, Cooley L, Hartwig JH, Noegel A, Schleicher M, et al. Filamins as integrators of cell mechanics and signalling. Nat Rev Mol Cell Biol 2001; 2: 138–45.

Thomas P, Bossan A, Lacour JP, Chanalet S, Ortonne JP, Chatel M. Ehlers-Danlos syndrome with subependymal periventricular heterotopias. Neurology 1996; 46: 1165–7.

Tu Y, Wu S, Shi X, Chen K, Wu C. Migfilin and Mig-2 link focal adhesions to filamin-and the actin cytoskeleton and function in cell shape modulation. Cell 2003; 113: 37–47.

Usuki F, Yamashita A, Higuchi I, Ohnishi T, Shiraishi T, Osame M, et al. Inhibition of nonsense-mediated mRNA decay rescues the phenotype in Ullrich's disease. Ann Neurol 2004; 55: 740–4.

van der Flier A, Sonnenberg A. Structural and functional aspects of filamins. Biochim Biophys Acta 2001; 1538: 99–117.

Wieck G, Leventer RJ, Squier WM, Jansen A, Andermann E, Dubeau F, et al. Periventricular nodular heterotopia with overlying polymicrogyria. Brain 2005; 128: 2811–21.